CHAPTER V

RESULTS AND DISCUSSION

In this Chapter, characteristics of the newly developed cyclen-ammonia and cyclen-water potentials have been reported. The structural properties of the solution have been discussed on the basis of the radial distribution functions, the corresponding integration numbers, distribution of coordination numbers, etc., in comparison with those of previous work. Before ending the Chapter, a solvation model for the solvation shell of a cyclen molecule in a water-ammonia solution has been proposed. Consequently, the contribution of the solution effect to the macrocyclic effect has been extrapolated.

5.1 Selection of a reliable basis set

In Table 5.1, characteristics of the *ab initio* calculations for various basis sets for cyclen-ammonia and cyclen-water are summarized. Excluding the STO-3G set, the same, expected conclusions for both systems can be drawn: the bigger the basis set, the longer the distance between the dimers, and the greater increase of stabilization energy ($-\Delta E$) and hence the computing time required. However, changes in the dipole moment of water and ammonia molecules are not in order.

Taking into consideration the STO-3G basis set, it is found in Table 5.1 that this basis set gives very good results for both systems. STO-3G is found to give the best dipole moments, compared with experimental data. Distances between the molecules are comparable with those for the big basis set, DZP while the time required is more than 60 times lower. Although the absolute values of the total energy (for both ammonia and water) is quite high (for example more than one Hartree higher than the DZP one) but the stabilization energies is good, relative to the biggest basis set given in Table 5.1. The compromise of these data lead to an easy decision without doubt, that the STO-3G is the suitable basis set for our systems.

Table 5.1 Optimal N-origin or O-origin distance (R in Å), dipole moment (μ in Debyes), total energy (E in Hartrees), stabilization energy (ΔE in kcal/mol) and CPU time (minutes) obtained from the SCF calculations with different basis sets.

basis set	NH_3		H_2O		cyclen	cyclen-NH_3		cyclen-H_2O		CPU time
	μ	E	μ	E	E	R	ΔE	R	ΔE	
STO-3G	1.79	-55.45408	1.73	-74.96293	-525.81849	3.1	-2.52	2.7	-5.52	5
3-21G	2.17	-55.87047	2.44	-75.58539	-529.31089	2.9	-8.88	2.6	-17.26	17
6-21G	2.16	-56.10208	2.41	-75.88787	-531.60689	3.0	-8.26	2.6	-16.57	18
6-31G	2.32	-56.16103	2.63	-75.98399	-532.02157	3.2	-5.29	2.7	-12.38	31
DZV	2.35	-56.17681	2.68	-76.00922	-532.09930	3.2	-3.90	2.8	-10.28	72
DZ	2.35	-56.17595	2.68	-76.00928	-532.10160	3.3	-3.86	2.8	-10.16	90
DZP	1.90	-56.20929	2.23	-76.04651	-532.40195	3.3	-3.05	2.9	-7.04	320
experiment	1.47[*]	-	1.74[**]	-						

*, ** values taken from ref. (46) and (64) for ammonia and water, respectively.

Additional conclusions could be again made concerning the use of basis sets. Since the way in which contractions are derived is quite complicated, bigger basis sets do not always give better results. Moreover, the choice depends upon the intended use of the basis set. Some of them are good for geometry and energies, and some are best for other properties, for example the dipole moment, polarizability, etc. For some calculations, a good representation of the inner (core) orbitals is necessary (for example, for properties required to analyze NMR spectra), while others require the best possible representation of valence electrons (65).

5.2   Intermolecular potential function

5.2.1 Cyclen-ammonia potential function

Table 5.2 shows the number of SCF data (N) included in the fit, standard deviations for the N points (σ), the number of testing points (N_{test}) used to test the previous function and the standard deviation for the N_{test} points (σ_{test}) for each iteration step. A reliable functional form for cyclen-ammonia is the Lennard-Jones form plus Coulombic terms, as shown in equation [4.4]. The standard deviation of the first iteration of 0.70 kcal/mol for N=300 indicates, at least, a good numerical fit. The σ_{test} of 0.30 kcal/mol for the additional 50 data points shows a good agreement between the cyclen-ammonia interaction energies predicted by the function and those obtained from the SCF calculations. The same situation is found for every iteration except step 4. In this step, the increase of σ_{test} to 1.14 kcal/mol is due to a contribution from the inclusion of the negative cyclen-ammonia interaction, which is in the direction along the N-H bond of cyclen. The SCF data near these functional groups were never included in the previous iteration steps. Up to step 7, consistency of the σ and σ_{test} has been obtained. Convergence of the fitting parameters for the last 3 steps is also detected. The final values of the fitting parameters are summarized in Table 5.3.

Table 5.2   Number of SCF-data points (N), standard deviation (σ in kcal/mol), number of testing points (N_{test}) and σ_{test} for each optimization step.

Step	N	σ	N_{test}	σ_{test}
1	300	0.70	50	0.30
2	350	0.68	50	0.23
3	400	0.67	50	0.36
4	450	0.65	50	1.14
5	500	0.72	50	0.28
6	550	0.70	50	0.37
7	600	0.68	-	-

Some comments could be made concerning the assignment of a negative or positive value to the fitting parameters. It is generally not possible in all cases to force A/r^6 to be negative and B/r^{12} to be positive, in order to represent, physically, attractive and repulsive interactions of the pair, respectively. One more reason for such assignments is to prevent the function from having *negative holes* at short distances, caused by a much higher slope B/r^{12} than for the other terms.

Table 5.3 Final optimized parameters for the interaction of nitrogen (a) and hydrogen (b) atoms (q_N=-0.46974, q_H=0.15658) of ammonia with cyclen molecule.

Atom	q_i (a.u.)	A (Å^6 kcal/mol)	B (Å^{12} kcal/mol)
(a)			
N	-0.31521	0.574661740221106E+04	0.598024965594606E+08
C	-0.00517	0.126685482049687E+03	0.502760578312786E+08
H_C	0.03273	-0.82760400785209E+03	0.308411086914211E+07
H_C	0.05944	-0.47853594120562E+03	0.828712652569475E+06
H_N	0.14120	-0.21717751170517E+04	0.527363815956959E+06
(b)			
N	-0.31521	-0.25517399503872E+04	0.160495232722942E+07
C	-0.00517	0.245217579630753E+03	0.553290806099452E+07
H_C	0.03273	0.141139597073117E+03	0.888396232381543E+05
H_C	0.05944	0.199423925753199E+03	0.147522377966090E+06
H_N	0.14120	0.775222682052077E+03	0.284710839871730E+05

In our cyclen-ammonia function, physical meaningful values of the coefficients are not achieved. This corresponds to what is observed in almost every case (66-68). However, a fall-off of the function at short distances, caused unwanted negative holes, does not occur, since the B/r^{12} terms for all atomic pairs are positive.

As mentioned before, the quality of the fit is indicated by the low standard deviation, but quality of the potential function obtained is judged by the positions of the minima, especially the global one. It is clearly seen that a good agreement between structural data obtained from Monte Carlo simulations depends on the shape of the function rather than on the absolute interaction energies. Sometimes a function with higher standard deviations may give more accurate results, especially in regard to intermolecular distances. Therefore, the most important factor indicating the quality of function is the correlation between the positions of the energy minima, ΔE_{SCF} and the ΔE_{FIT}. To examine this characteristic, the stabilization energies obtained from the quantum chemical calculation were plotted versus those obtained from the function with parameters summarized in Table 5.3 and in the directions indicated by ϕ and θ (see Figure 4.2). For all three curves, one of the N-H bond of the ammonia molecule is in the selected direction. The energies extracted from both sources are monitored in Figure 5.1. The difference in the position of the minima is almost negligible.
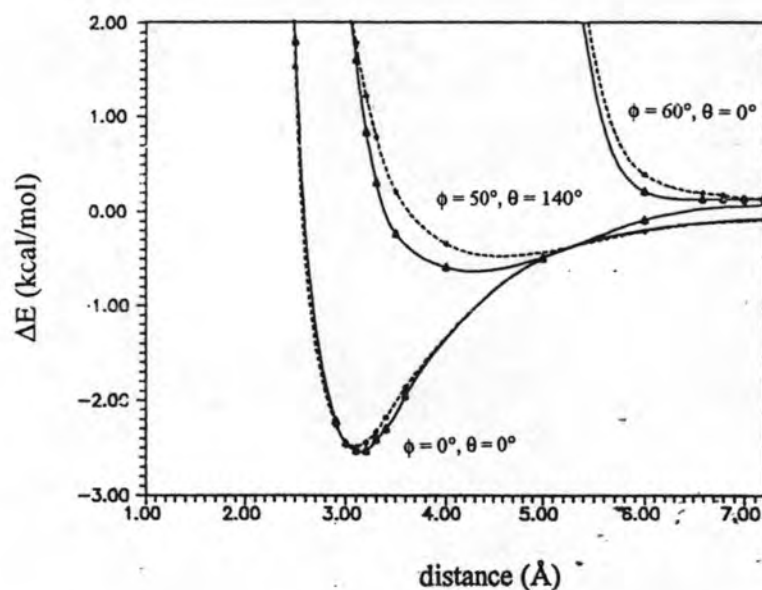
Figure 5.1   The stabilization energies obtained from the STO-3G *ab initio* calculations (solid line) and from the cyclen-ammonia function shown in equation [4.4] (dashed line) with the fitting parameters given in Table 5.3 versus the N-origin distance (Figure 4.2).

Further confirmation of the quality of the fit is given by comparing ΔE_{SCF} and ΔE_{FIT}, as displayed in Figure 5.2. Perfect agreement would have implies a straight line of unit slope, and the scatter about this line gives a graphical measure of the quality of the fit. The plot indicates a good agreement between both data, especially for the attractive ranges, which is important for prediction of the simulation results.
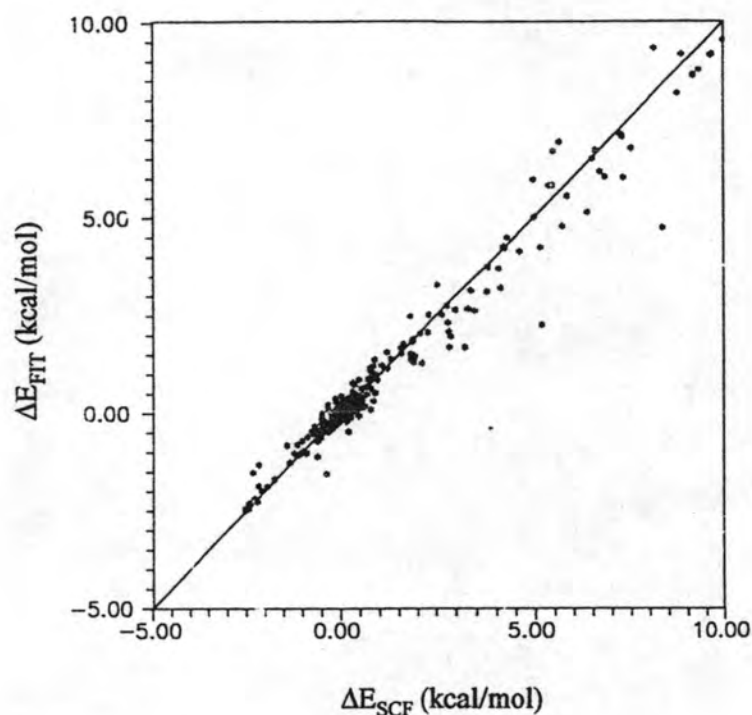

Figure 5.2   Comparison of the stabilization energies from the STO-3G *ab initio* calculations, ΔE_{SCF}, and from the cyclen-ammonia potential function, ΔE_{FIT}, shown in equation [4.4] with fitting parameters given in Table 5.3.

5.2.2 Cyclen-water potential function

The HR potential:

As outlined in section (4.3.2), unwanted minima in the HR cyclen-water potential (63) were detected (Figure 5.3). Potential curves where the water

molecule lies in the optimal direction (see Figure 4.3a), in the direction where the unwanted minimum occurs (see Figure 4.3b) and in the direction along the N-H bond of cyclen, where hydrogen bonding is expected to take place, were plotted. The interaction energies were computed from both the SCF calculation using the STO-3G basis set and the HR cyclen-water potential. In all cases, the HR dimerization energies are more than 100% lower than the STO-3G ones. Therefore, the HR cyclen-water potential gives too attractive interaction, especially in positions near the local energy minima of the chemically important configurations. The overestimated attractions and the shift of the distances to the minima could surely lead to wrong simulation results, both in terms of positions of the peaks in the radial distribution function, and consequently, in the coordination numbers. The discrepancy of the HR potential, despite its shortcomings caused by the numerical fitting, indicates a methodical limit of the GLO basis function in prediction of the cyclen-water geometry.
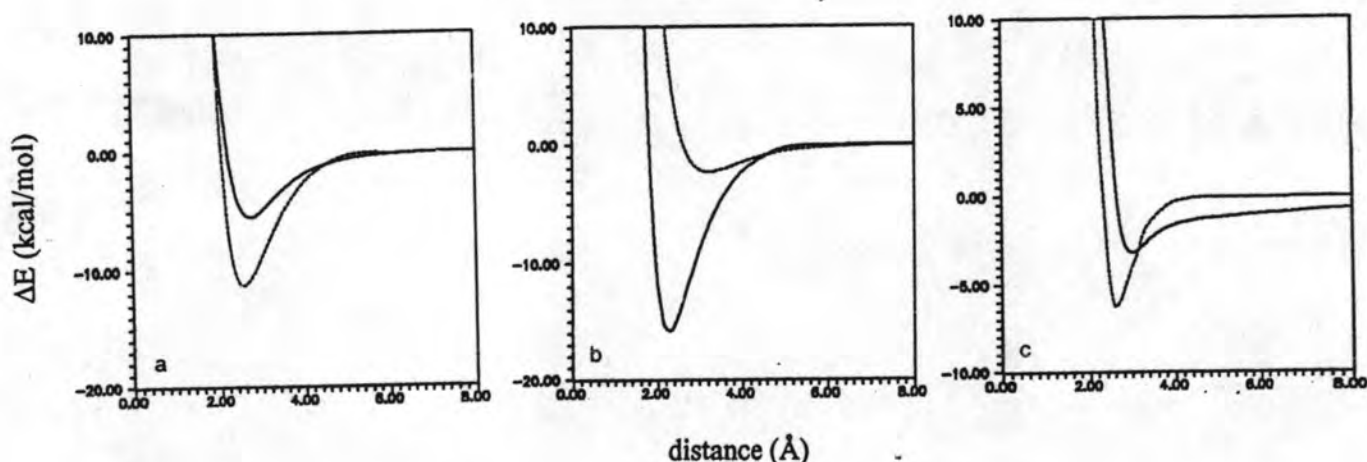
Figure 5.3   Potential energy curves obtained from the HR potential (dashed lines) and from the *ab initio* calculations using the STO-3G basis set (solid lines) where water molecule lies in:
   a)   the optimal direction (Figure 4.3a),
   b)   the direction where the unwanted minimum occurs (Figure 4.3b) and,
   c)   the direction along the N-H bond of cyclen.

The newly developed potential:

In similarity to the cyclen-ammonia function, interaction energies between cyclen and water, ΔE_{SCF}, have been fitted to an analytical potential of the form

$$\Delta E(L, W) = \sum_{i=1}^{3}\sum_{j=1}^{32} \frac{A_{ij}^{ab}}{r_{ij}^6} + \frac{B_{ij}^{ab}}{r_{ij}^{12}} + \frac{C_{ij}^{ab}}{r_{ij}^4} + q_i q_j [\frac{1}{r_{ij}} + \frac{1}{r_{ij}^2}] \qquad [5.1],$$

where the related variables and constants are equivalent to those of equation [4.4].

The final values of the fitting parameters are summarized in Table 5.4. Some selected potential curves for both ΔE_{SCF} and ΔE_{FIT} are plotted in Figure 5.4 and their correlation is illustrated in Figure 5.5.

Table 5.4 Final optimized parameters for the interaction of oxygen (a) and hydrogen (b) atoms (q_O=-0.36633, q_H=0.18316) of water with cyclen molecule.

Atom	A (Å^6 kcal./mol)	B (Å^{12} kcal/mol)	C (Å^4 kcal/mol)
(a)			
N	-0.181044934098700E-01	0.231435867631958E+06	0.3302324526184O5E+02
C	-0.90884264451195E+02	0.207043930079774E+07	0.405301193769179E+02
H_C	-0.84689490494778E+03	0.319998117747856E+06	0.607378049513265E+01
H_C	-0.157559977561574E-01	0.221200432754649E+04	0.864485602862903E+01
H_N	-0.421048677015495E-01	0.773339642093241E+03	0.202690175176823E+02
(b)			
N	-0.30807238686515E+02	0.788451247667679E+02	0.175571605758651E+02
C	-0.10529913191582E+03	0.591790266347744E+05	0.159690683732704E+02
H_C	-0.22282668793251E+00	0.477655357660867E+04	0.203789205031606E+02
H_C	-0.450320034306229E-02	0.33851623386268E+00	0.172227076875677E+02
H_N	-0.109231327935363E-01	0.157351606673764E+04	0.157515252211102E+02

As only absolute values were allowed for the parameters, A and B represent attractive and repulsive interactions between atoms i and j, respectively, while C corresponds to either a repulsive or attractive interaction, depending on the sign of q_i and q_j. The third term, C_{ij}^{ab}/r_{ij}^4, is taken into account in order to obtain a better numerical fit. The second Coulombic term is included not only to improve the numerical fit, but also to make possible a distance dependence of the net cyclen and water atomic charges. The basic idea is that when a water molecule moves close to the cyclen molecule, the atomic charges should vary as a function of the distance and the orientation of water relative to cyclen, due to mutual polarization effects. This approach was successfully used for water-amino acid interactions (59-62).
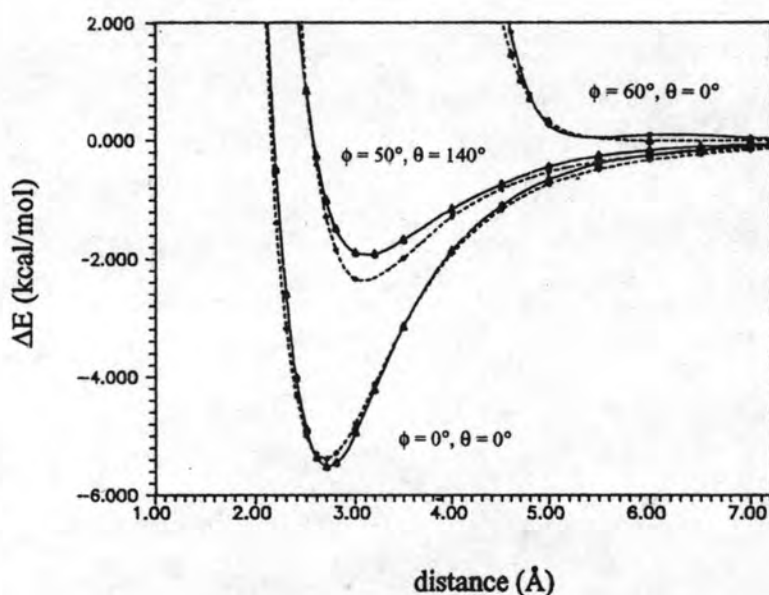
Figure 5.4   The stabilization energies obtained from the STO-3G *ab initio* calculations (solid line) and from the cyclen-water function shown in equation [5.1] (dashed line) with the fitting parameters given in Table 5.4 versus the O-origin distance (Figure 4.2).

It is apparent that the fit is rather good for all important low lying energy points but gets gradually worse, as being moved towards the repulsive energy region. Distances to the minima for all curves of the ΔE_{SCF} and the ΔE_{FIT} are identical. In addition, a negative hole in the ΔE_{FIT} for short distances surely

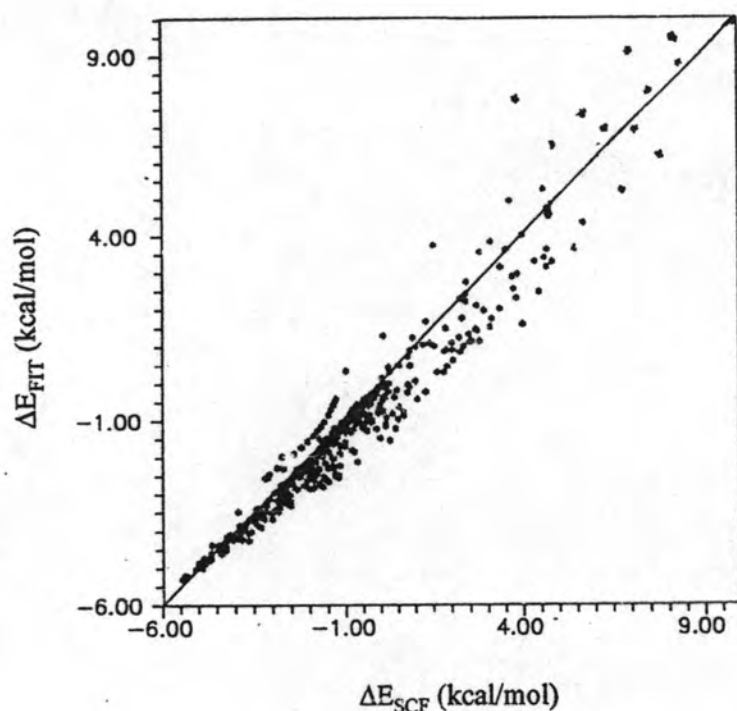does not occur, since the contribution from the second term of equation [5.1] is always positive.

Figure 5.5   Comparison of the stabilization energies from the STO-3G *ab initio* calculations, ΔE_{SCF}, and from the cyclen-water potential function shown in equation [5.1] with the fitting parameters given in Table 5.4, ΔE_{FIT}

Basis set superposition error:

The results of the *ab initio* calculations including the Boys-Bernardi counterpoise correction using the STO-3G and the DZP basis sets were collected in Table 5.5 and plotted in Figure 5.6.

As expected, the calculations for both basis sets without the correction cause too low a stabilization energy of the dimer. The smaller the basis set, the higher the BSSE obtained. The STO-3G global minimum is shifted from -5.52 kcal/mol and 2.70 Å to -2.97 kcal/mol and 3.00 Å. The corresponding changes for the DZP are from -7.04 kcal/mol and 2.90 Å to -5.49 kcal/mol and

3.00 Å. Since the decision has been already made in section (5.1) that STO-3G is the best basis set for this study, what has to be considered in this step is whether the counterpoise correction has to be applied. Suppose that the DZP data with the correction is the best one, among the four possible combinations of STO-3G and DZP with and without the BSSE correction, as displayed in Table 5.5. Difficulties then arise, the distance to the global minimum obtained from the STO-3G set with a BSSE correction is correct while the corresponding interaction energy of -2.97 kcal/mol is too high compared with -5.49 kcal/mol from the DZP set with the correction. Without the correction, the STO-3G stabilization energy is correct, while the distance is 0.30 Å shorter. Since the potential curves near to the minima are quite broad, the shift of the distance is within the KT limit, where K is the Boltzmann constant and T denotes temperature in degrees Kelvin, while the energy shift of 2.52 kcal/mol (the difference between ΔE_{BSSE} for DZP and STO-3G basis sets) is outside limit (0.6 kcal/mol). Therefore, the STO-3G basis set has been selected to be used in the SCF calculations without applying the BSSE correction.

Table 5.5   Binding energies with (ΔE_{BSSE}) and without BSSE (ΔE) in kcal/mol at different O-origin distances (R in Å) for the optimal directions of the cyclen-water configuration given in Figure 4.2, calculated using a) the STO-3G basis set,

R	ΔE	ΔE_{BSSE}	R	ΔE	ΔE_{BSSE}
1.90	11.32	23.52	3.00	-4.94	-2.97
2.00	6.31	17.05	3.20	-4.21	-2.96
2.20	-0.49	7.65	3.50	-3.15	-2.55
2.30	-2.59	4.44	4.00	-1.85	-1.71
2.40	-4.01	2.01	4.50	-1.09	-1.07
2.50	-4.89	0.22	5.00	-0.65	-0.66
2.60	-5.36	-1.05	5.50	-0.39	-0.41
2.70	-5.52	-1.92	6.00	-0.24	-0.26
2.80	-5.45	-2.48	7.00	-0.10	-0.12
2.90	-5.25	-2.81	8.00	-0.04	-0.01

b) the DZP Basis set.

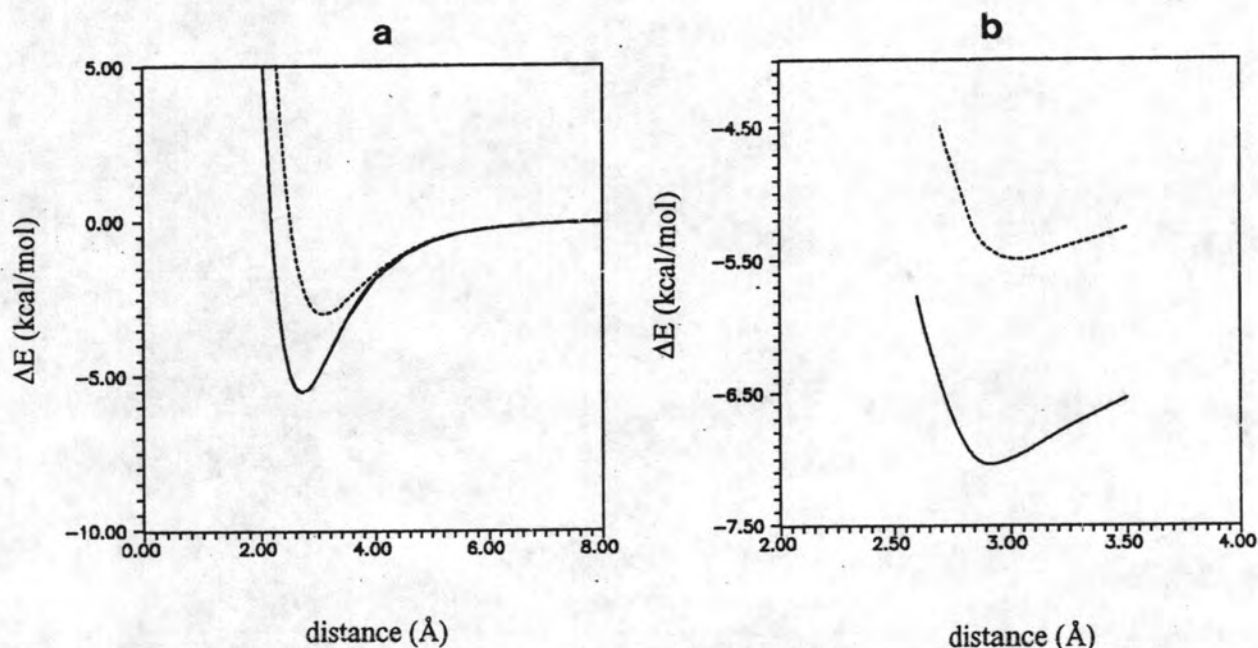| R	ΔE	ΔE_{BSSE}	R	ΔE	ΔE_{BSSE}
2.70	-6.43	-4.50	3.00	-7.00	-5.49
2.80	-6.86	-5.03	3.10	-6.82	-5.42
2.90	-7.04	-5.39	3.20	-6.54	-5.26

Figure 5.6   The cyclen-water stabilization energy for the optimal direction (see Figure 4.3a) as a function of the O-origin distance, calculated with (dashed line) and without BSSE (solid line) using
a) the STO-3G basis set, and b) the DZP basis set (only area close to the global minimum).

5.3   Solvation structure of the cyclen molecule in an aqueous ammonia solution

Before entering into a detailed discussion of structure properties of the solution, the global stabilization energies and distances were extracted from

the pair potentials and summarized in Table 5.6. The corresponding configurations of each solvent pair are depicted in Figure 5.7. This information is primarily required for interpreting and understanding the obtained results.

Table 5.6 The lowest stabilization energy (kcal/mol) and the corresponding distance for each solute-solvent and solvent-solvent.

solvent-solvent	r (Å)	ΔE	solute-solvent	r (Å)	ΔE
water-water	2.90	-5.69	cyclen-water	2.70	-5.51
water-ammonia	3.10	-7.29	cyclen-ammonia	3.10	-2.53
ammonia-ammonia	3.30	-1.54			
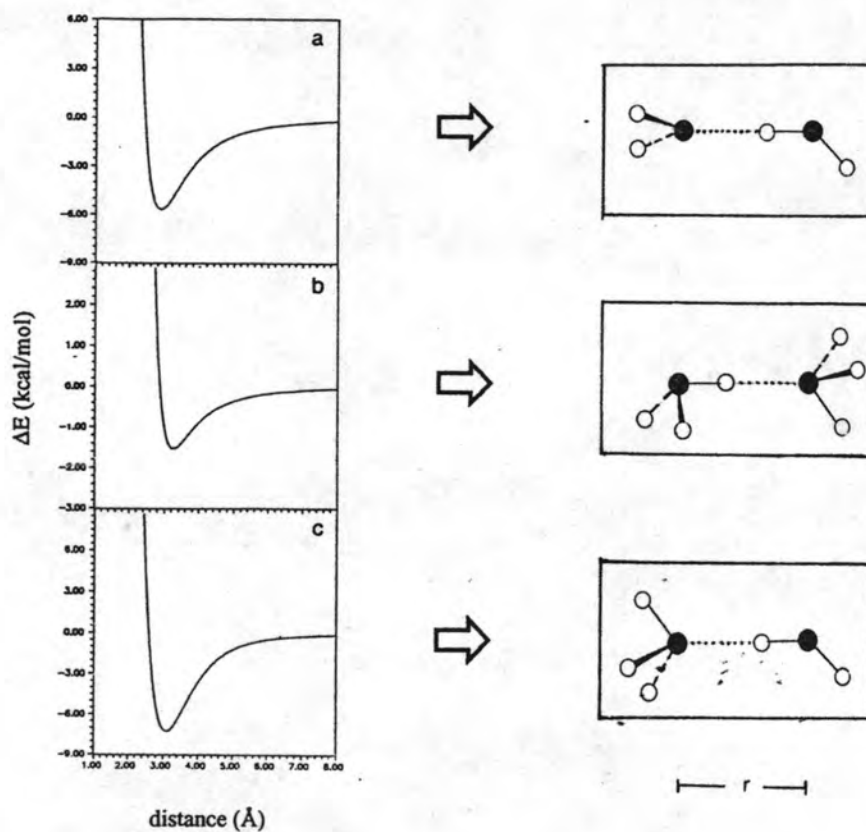
Figure 5.7 The solvent-solvent configurations where global interaction energies (Table 5.6) occur for

a) water-water,   b) ammonia-ammonia and   c) water-ammonia interactions
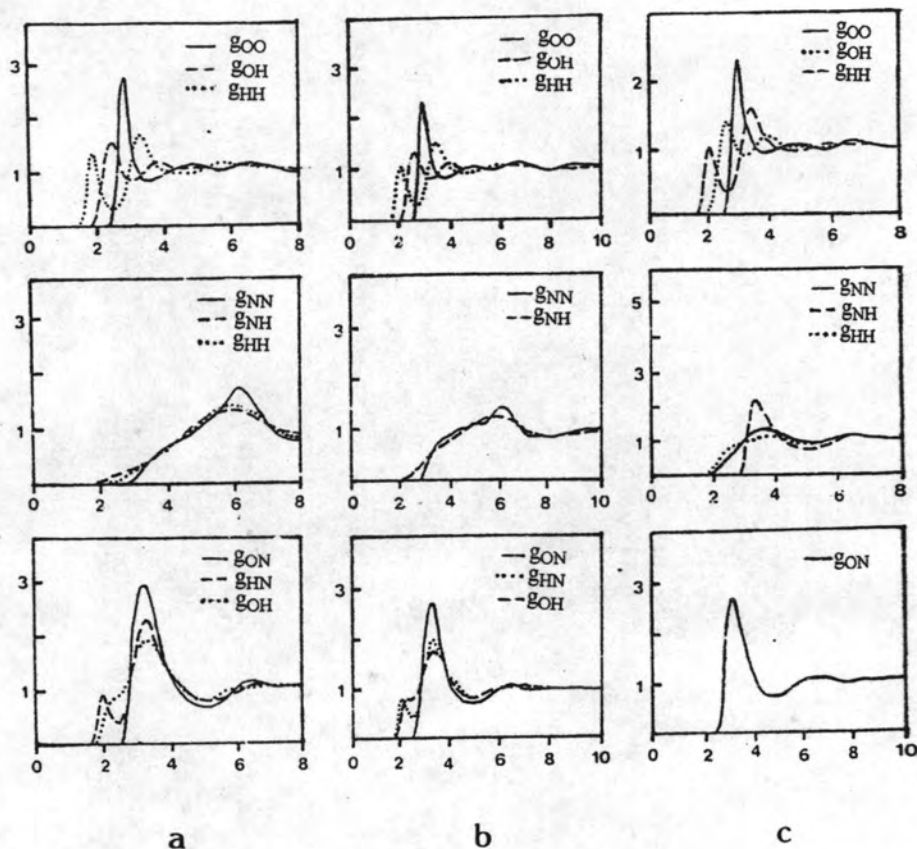
Figure 5.8 H$_2$O/H$_2$O (top), NH$_3$/NH$_3$ (middle) and H$_2$O/NH$_3$(bottom) radial
distribution functions obtained from the Monte Carlo simulations of
18.45 mol% of aqueous ammonia solution with
a) one cyclen molecule, b) one Li(I), and c) without solute
(the bottom g$_{NO}$(r) taken from ref. (58) is the experimental results).

5.3.1 Solvent Structure

In order to investigate structural changes of solvent molecules in the
dilute solution of cyclen, the atom-atom RDFs for H$_2$O/H$_2$O, H$_2$O/NH$_3$ and

NH_3/NH_3 have been evaluated and plotted in Figure 5.8. The experimental $g_{NO}(r)$ for 18.45 mol% aqueous ammonia and the simulation results for one Li(I) in the equvalent solvent, which is assumed to display identical structure properties as those of solvent, have been also given for comparison. The results show that there are no major differences between the solvent structure around the cyclen molecule and those of aqueous ammonia without cyclen, except for a slightly lower amplitude at some distances. This small deviation is due to the fact that in the presence of the large cyclen molecule, the structure of the solvent in the vicinity of the ligand will be significantly altered, leading to a decrease in the number of solvent molecules in the ideal bulk solvent orientation. The same results have also been reported for a dilute solution of cyclen in water (63) and a water-methanol mixture (69), and also for dilute cations in water (70-73). The characteristics of the pronounced peaks in the RDFs are summarized in Table 5.7.

Table 5.7 Characteristic values of the radial distribution functions for a cyclen molecule in a 18.45 mol% aqueous ammonia solution. R_{M1} and r_{m1} are the distances in Å for the first maxima and minima of $g_{xy}(r)$, respectively. n_1 is the average coordination number integrated up to r_{m1} of the first shell.

xy	R_{M1}	r_{m1}	n_1
H_2O-H_2O			
O-O	2.80	3.55	4.3
O-H	1.90	2.55	1.7
H-H	2.45	3.10	4.9
NH_3-NH_3			
N-N	6.20	7.75	11.4
N-H	5.70	7.90	35.7
H-H	5.80	8.20	39.2
H_2O-NH_3			
O-N	3.25	4.95	3.3
O-H(NH_3)	3.30	4.95	9.9
H(H_2O)-N	2.15	2.45	1.2

Water-water:

As shown in Figure 5.8 (top) and Table 5.7, the first pronounce peak in $g_{OO}(r)$ is at 2.80 Å. The second and third peaks have been also detected. The hydrogen bonding, which is a typical characteristic of water, has been exhibited by the small sharp peak of the $g_{OH}(r)$ centered at 1.90 Å. All the mentioned characteristics are the same as those of a very dilute solution of Li(I) in 18.45 mol% aqueous ammonia (71) and of pure water (74). The first shell coordination numbers, integrated up to the first minimum of $g_{OO}(r)$ is 4.3. This number is the same as those obtained for Li(I) (71), Na(I) (72), and Mg(II) (73) in 18.45 mol% aqueous ammonia. It is, as expected, reduced from 6 for pure water because the other two coordination sites are replaced by ammonia molecules.

Ammonia-ammonia:

No significant difference is found between the ammonia-ammonia RDFs calculated from this study (Figure 5.8a, middle) and from the equivalent solvent with Li(I) (Figure 5.8b, middle). They were completely changed in comparison with those of the pure solvent (Figure 5.8c, middle). The distortion of the RDFs could be related to the presence of only a small number of ammonia molecules in the simulation box. In addition, due to a weak ammonia-ammonia interaction energy (Table 5.6), their first-shell coordination sites would be easily replaced by water molecules to form a hydrogen bond of the type H_3N-----HOH, as shown in Figure 5.7c.

Water-ammonia:

All the characteristics of the water-ammonia RDFs for all cases, even those obtained experimentally, are almost identical. The first pronounced $g_{NO}(r)$, and hence $g_{ON}(r)$, peaks are centered at 3.25 Å. The hydrogen bond between water and ammonia molecules in the configuration given in Figure 5.7c has been clearly revealed by the small and sharp first $g_{NH}(r)$ peaks (Figure 5.8a-5.8b, bottom). A small contribution from the hydrogen bond of type H_2O---HNH_2

also appears as a small shoulder at about 2.5 Å for $g_{OH}(r)$ (Figures 5.8a and 5.8b, bottom).

5.3.2 Water structure around the cyclen molecule

Overview:

Since the cyclen-water stabilization energy evaluated from the pair potential is two times lower than that of cyclen-ammonia (Table 5.6), the cyclen molecule was expected to be solvated, in the first hydration shell, by water. Therefore, many investigated quantities were restricted to this shell. In similarity with the previous work (63), space around the cyclen molecule was divided into three regions; top, side and plane. Top corresponds to the conical volumes enclosed by rotating a 45° vector, starting from the molecular centre, around the ± Z-axis (see Figure 5.9) and side corresponds to the volume below that vector. Inside this side region a cylinder of height ± 1 Å along the Z-axis was defined as the plane region.
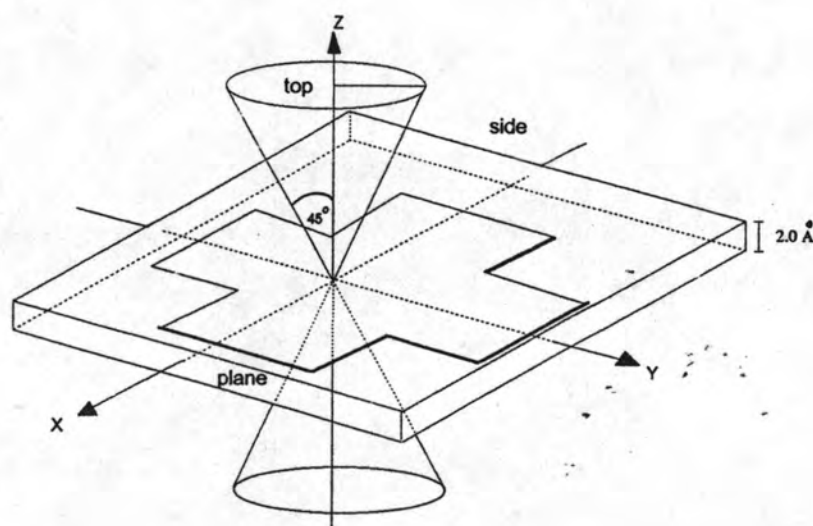
Figure 5.9   Orientation of the cyclen molecule in the coordinate system, indicating top, side and plane regions.

For all the radial distribution functions between atoms or group of atoms of cyclen and atoms of solvent, the notations $g_{xy}(r)$ have been used, where x can be either the ligand atoms or the centre of mass of cyclen for the following regions: E (entire system), T (top), S (side) and P (plane), and y denotes the O/H atoms of water or N/H atoms of ammonia molecule.

After 7 million configurations of the simulations, energetic equilibration of the system was reached. The distributions of individual and of both solvents, taken from one out of several million configurations, have been plotted separately in Figure 5.10. Each type of solvent molecules is well scattered all over the basic box. Homogeneity of both solvents is also well revealed. Such plots are important and useful in order to prevent the system, especially one with more than one species, from having local energy equilibration. If the starting configurations were far from homogeneity, several million configurations would have been required because it was found that for each million moves, displacement of each molecule of only some Angstroms from its original position normally takes place. It has been founded, as expected, that water molecules can approach closer to the cyclen molecule (Figure 5.10a) than ammonia (Figure 5.10b). This finding was again confirmed by the RDFs from the molecular centre of cyclen to the O atom of water and N atom of ammonia, as given in Figure 5.11. The first water molecule was detected at 2.8 Å away from cavity of cyclen (molecular center) while the first ammonia was found at 5.0 Å.

a   b   c
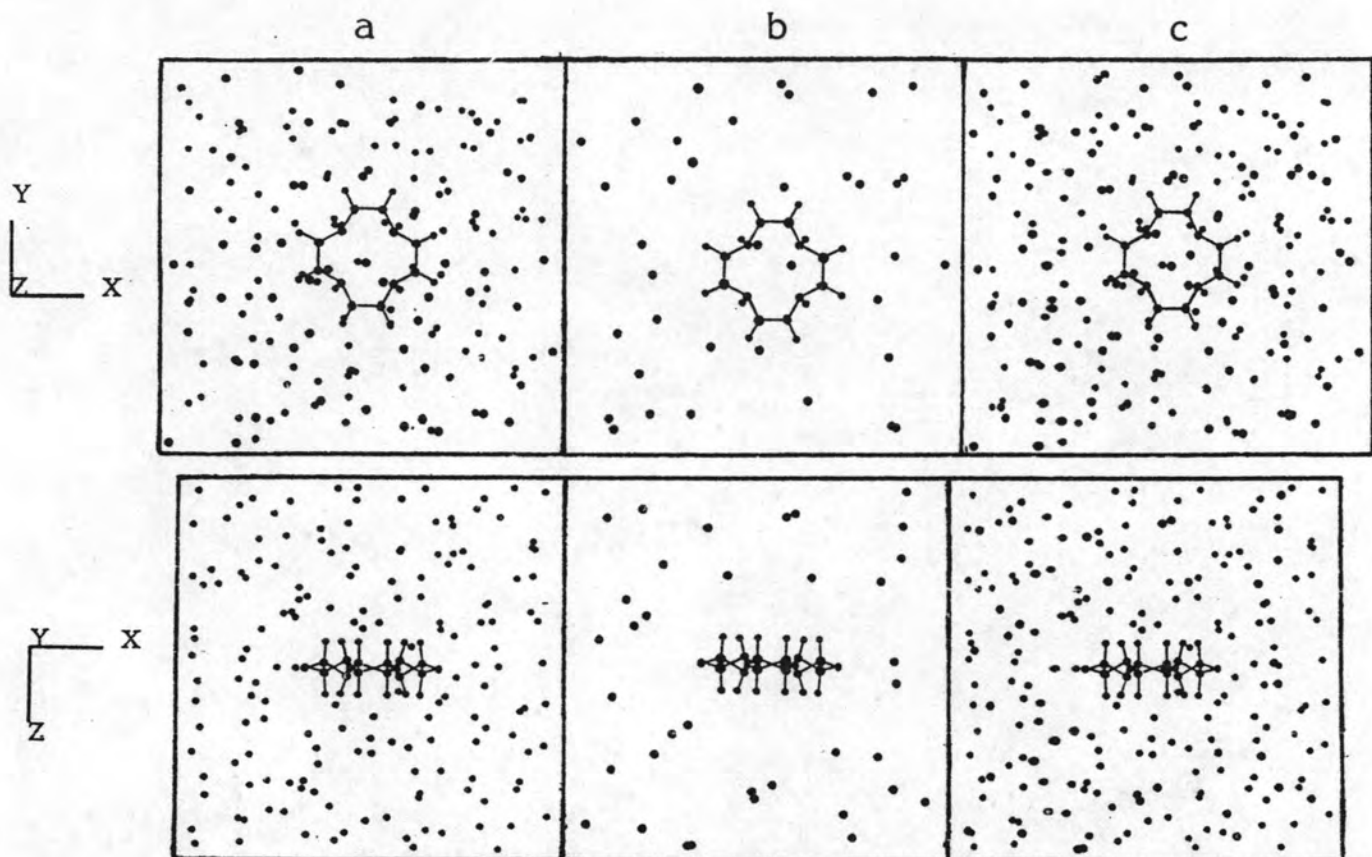
Figure 5.10   Distributions of a) water, b) ammonia and c) both solvent molecules taken from one out of several million configurations of a cyclen molecule in a 18.45 mol% aqueous ammonia solution.
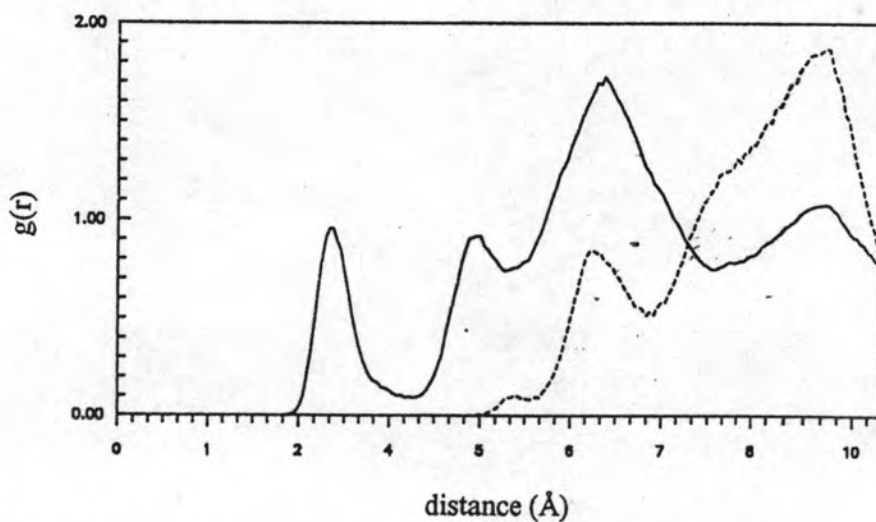
Figure 5.11   The E-O (solid line) and E-N (dashed line) radial distribution functions.

The solvent exchange:

As mentioned in section (4.3.3), the simulations had to be carried out for 35 million configurations due to the detection of the asymmetric distribution of two water molecules above and below the cyclen's cavity. The RDFs regarding the distribution of O and H atoms of water around the center of mass of cyclen, $g_{EO}(r)$ and $g_{EH}(r)$, respectively, for the 8-35 millionth configurations have been calculated separately and plotted in Figure 5.12.

Considering $g_{EO}(r)$ for the 8th million, it shows the first broad peak ranging from 2.4 Å to 3.2 Å. The running integration numbers of about 1.0 up to 3.2 Å and of about 2.0 up to 4.2 Å indicate that one water molecule (W1) is situated very close to the cyclen's cavity under the above mentioned peak and the other one (W2) is between 3.2 Å and 4.2 Å. In the 9th and 10th millions, W2 was moved from this solvation shell. The 11th million, W2 moved back again to the shell, and stayed there their until the 15th million. It escaped again in the 16th and 17th millions, but returned to the shell between the 18th and 20th million.

In the 21st million, both water molecules were kept as the nearest solvation shell but orientation of W2 was altered. This conclusion is indicated by the equivalent numbers of O and H atoms of water centered under the first peaks of $g_{EO}(r)$ and $g_{EH}(r)$, respectively. The integration curves of the 8th and the 20th millions are almost parallel, unlike those of the 21th million. The observed behavior can be understood from the global stabilization energies of the pair given in Table 5.6.

As outlined before and as depicted in Figure 5.10, water molecules were distributed homogeneously in the simulation box, while ammonia molecules, which display much lower dimerization energies with cyclen than water, were scattered only in the outer sphere far from the cyclen. W1 and W2 are held in place by the binding energy of -5.5 kcal/mol and are opposed by, somehow, equivalent water-water and slightly stronger water-ammonia interactions, situated in the outer shell (see Table 5.6). The move of W2 from and to the area of the first $g_{EO}(r)$ peak would be related to this fact.
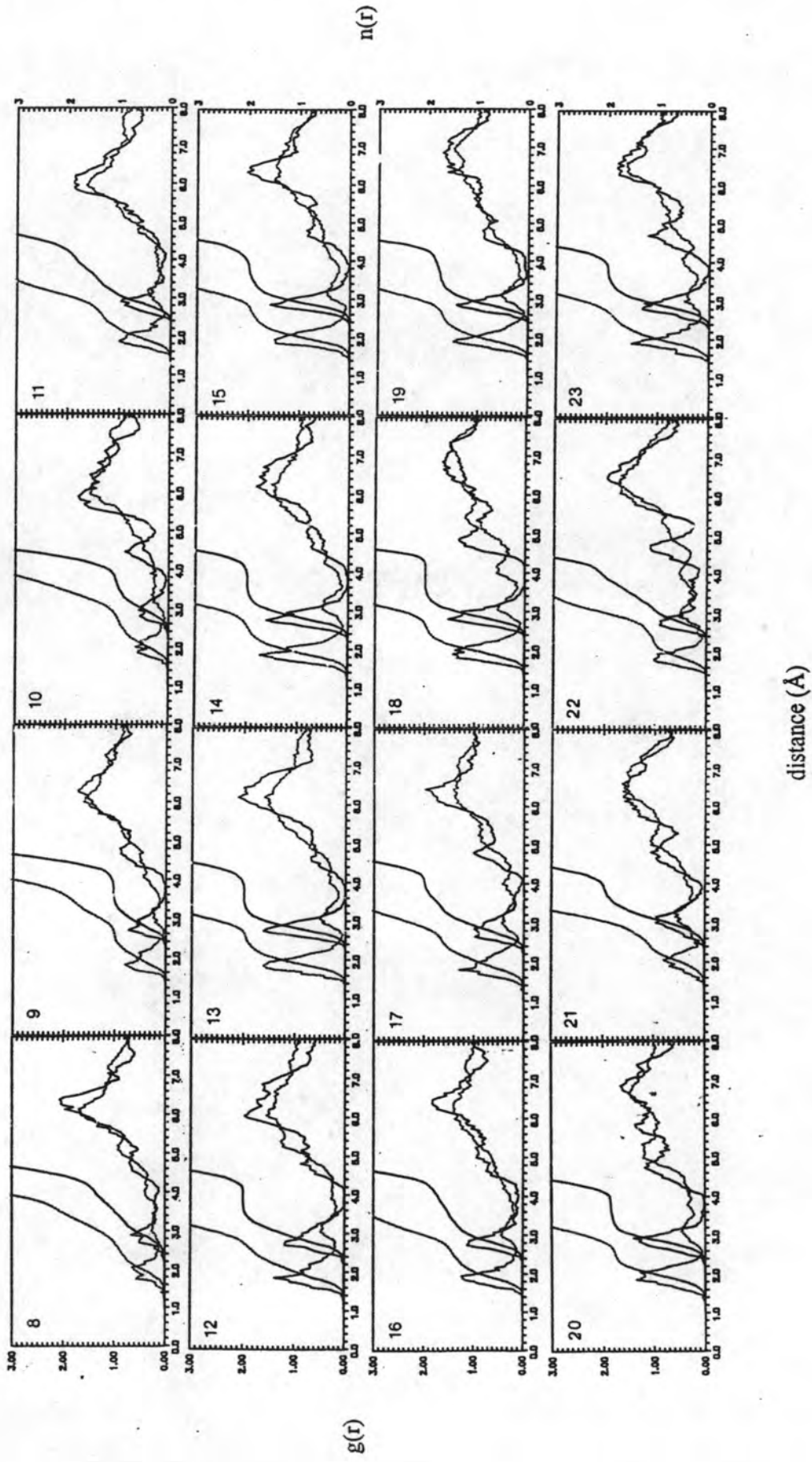
57

Figure 5.12 The E-O (solid line) and E-H (dased line) radial distribuion functions for the 8th-35th million configurations.
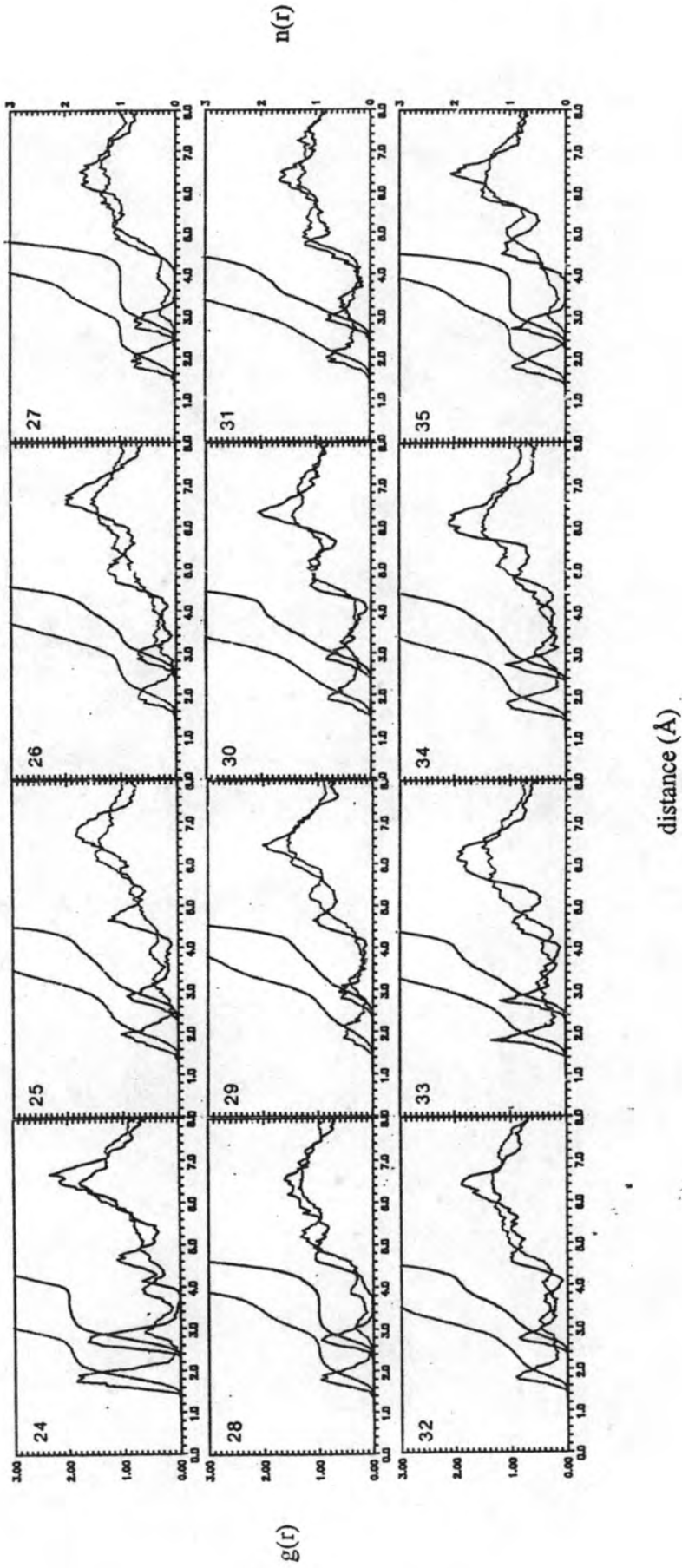
n(r)

distance (Å)

g(r)

Figure 5.12 (continued)

Figure 5.13 shows the distance between the oxygen atom of water and the center of mass of cyclen versus the number of configurations. Calculations have been done separately for W1, W2 and any other water molecules situated not more than 4.2 Å from the cavity of cyclen. It has been found that W1 was tightly bound to cyclen's cavity for the whole run (35 million configurations). The O1 (of W1)-origin distances fluctuate in a narrow range between 2.20 Å and 3.40 Å, except at the end of the 15th million and the beginning of the 16th million. W2 was more flexible and could escape, in some certain periods, *i.e.*, the distance to the center of cyclen was more than 4.2 Å (Figure 5.13b). For instance, W2 disappeared in the 8th, 26th and 28th millions (Figure 5.13b). Then, coordination numbers under the first peak of the corresponding millions (Figure 5.12) were consequently decreased. During 28 million configurations, no more water molecule other than W1 and W2 approached to a distance less than 4.2 Å, even for the configurations where W2 was gone.

Since solvent exchange behavior has been detected from one set of one million configurations to another, some questions were then arose. How many configurations have to be taken into consideration and when should the simulation stop?

Our conclusion is that one should include as many configurations as possible until periodicity in the RDFs is reached. For instance, starting from the 9th million, one water molecule lies close and points one hydrogen atom towards the cyclen's cavity. Simulations have to be carried out up to the 27th, 28th or 35th million when either the same or an other water molecule has returned to occupy its original configuration. In addition, the shape of the whole curves should not change much. A decision has been made, in this study, to average the RDFs and the corresponding integration numbers from all 28 million configurations. Due to methodological limits, the other properties reported in this work are investigated from the last three million configurations.
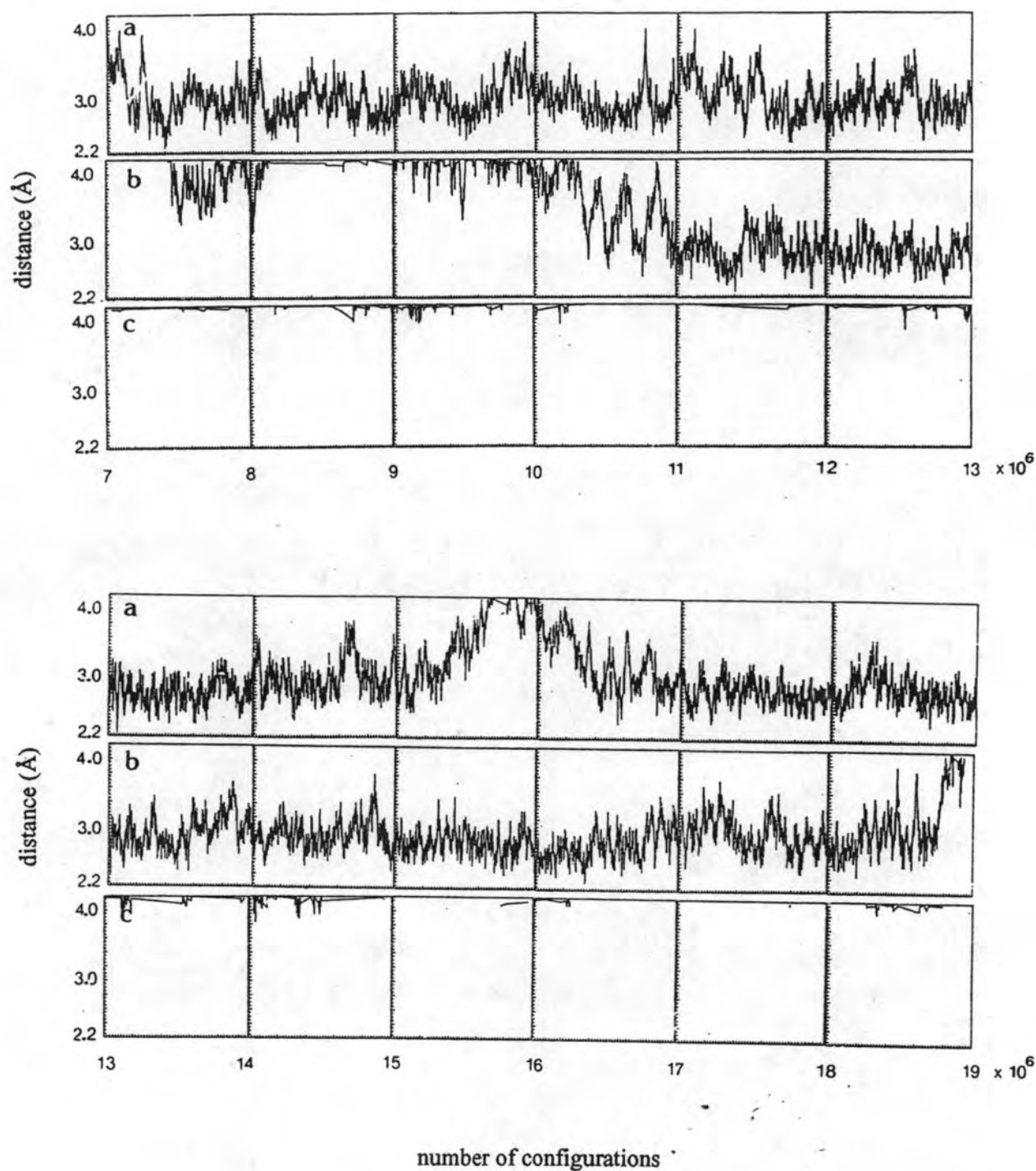
Figure 5.13   Distances between the oxygen atom of water and the center of mass
of cyclen versus number of configurations for
a) W1, b) W2 (for details see text), and c) any water molecules
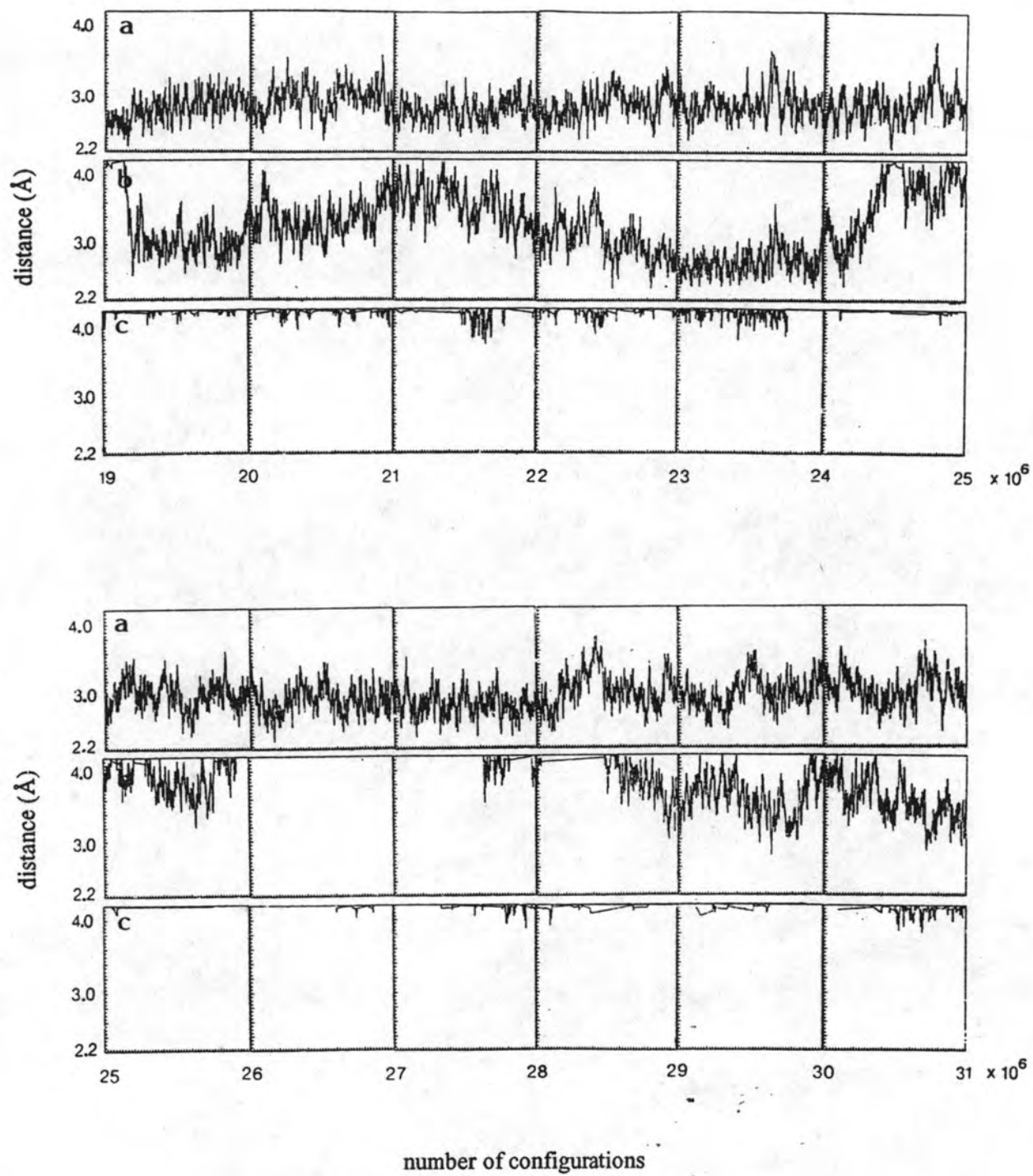which approach closer than 4.2 Å to the cyclen's cavity.

Figure 5.13   (continued)

Nearest neighbors:

In Figure 5.14, the radial distribution functions referring to the center of mass of cyclen, namely, top, side, and plane regions compared to the entire molecule and the corresponding running integration numbers are depicted. Characteristic data for these RDFs are given in Table 5.8

The E-O RDF shows a sharp first peak centered at 2.80 Å, with a corresponding integration number of 1.7. An identical peak, in terms of peak height, peak position and integration numbers, is found only in the top region. These waters were tightly coordinated to the cyclen's cavity. They apparently did not contribute to the other regions, side and plane. The orientation of these water molecules are indicated by the appearance of the first $g_{EH}(r)$ peak at 1.9 Å and the integration number up to the first minimum of 1.5; they are in the configuration where the global energy minimum occurs (Figure 4.3a). The average of 1.7 water molecules means practically, as demonstrated before, that the cyclen molecule was solvated closely by two water molecules, the tightly bound (W1) and the movable (W2) ones. W2 is often found (Figure 5.13b) to move from and to the region of the first $g_{EO}(r)$ peak. Therefore, the ratio of times when the cyclen molecule is solvated by one and two water molecules is 1:2.3. In conclusion, W1 and W2 are considered to be the nearest neighbors of cyclen.

Table 5.8 Characteristic values of the radial distribution functions for a cyclen molecule in 18.45 mol% aqueous ammonia solution. R_{Mi}, r_{mi} are the distances in Å for the *i*th maxima and minima of $g_{xy}(r)$, respectively. n_i is the average coordination number integrated up to r_{mi} of the *i*th shell.

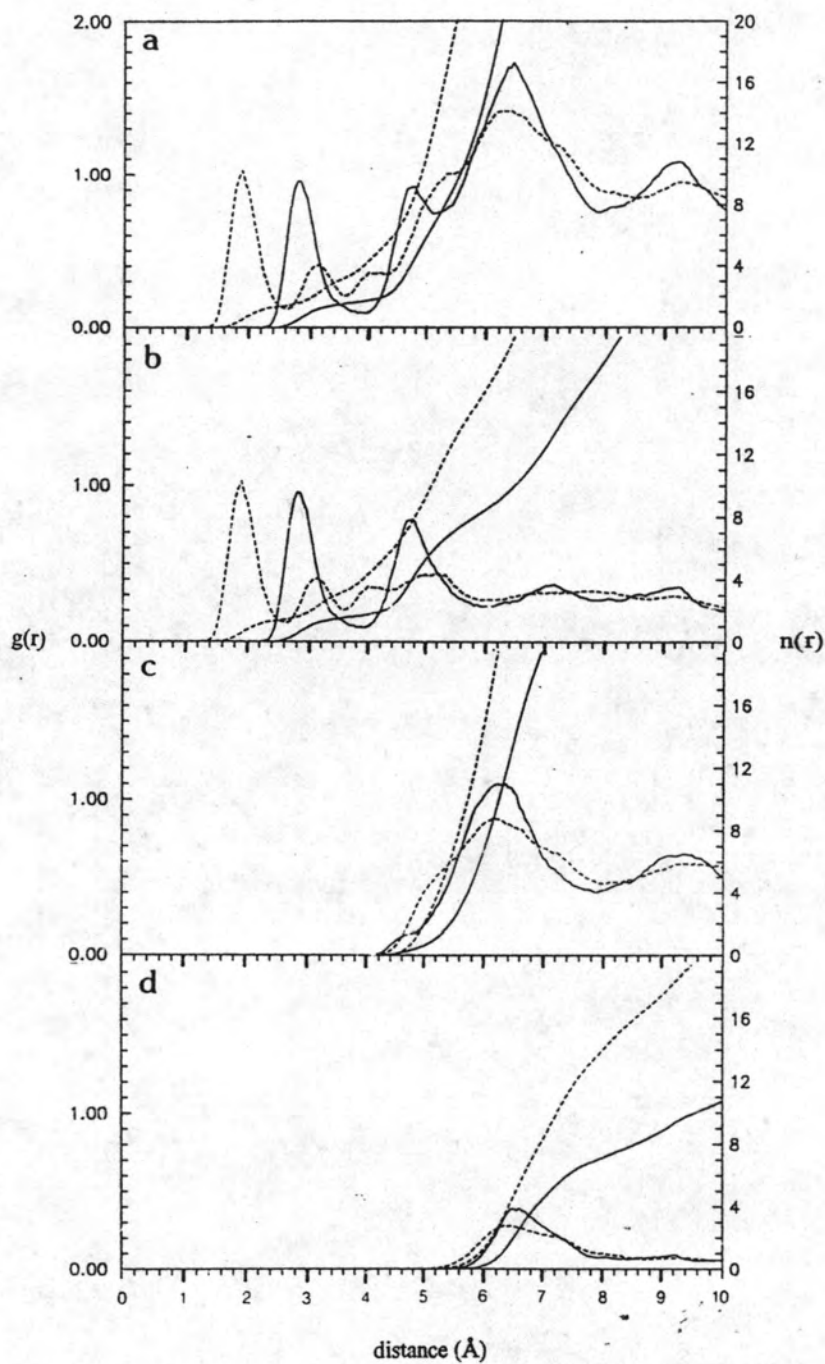| xy	R_{M1}	r_{m1}	n_1	R_{M2}	r_{m2}	n_2	R_{M3}	r_{m3}	n_3
E-O	2.80	3.80	1.7	4.75	5.15	6.9	-	-	-
E-H	1.90	2.65	1.5	3.15	3.55	3.2	4.00	4.25	5.3
T-O	2.80	3.80	1.7	-	-	-	-	-	-
T-H	1.90	2.65	1.5	3.15	3.50	3.2	4.00	4.35	5.7
N-O	3.05	3.30	0.8	3.75	4.00	2.6	-	-	-
N-H	2.45	2.55	0.5	-	-	-	-	-	-
H_N-O	2.75	3.65	2.7	-	-	-	-	-	-
H_N-H	2.35	3.40	4.4	-	-	-	-	-	-

Figure 5.14   Radial distribution functions and corresponding running intergration
numbers from O (solid line) and H (dashed line) of water to the
centre of mass of cyclen in the following regions:

a) entire,   b) top,
c) side, and   d) plane.

In order to evaluate the detailed orientation of W1 and W2, the distribution of the angle β, formed by a vector pointing from the oxygen atom of the water molecule, be above or under the molecular plane, to center of mass of cyclen and the dipole moment vector has been examined. The calculations have been done separately for W1 and W2. The results are displayed in Figure 5.15.
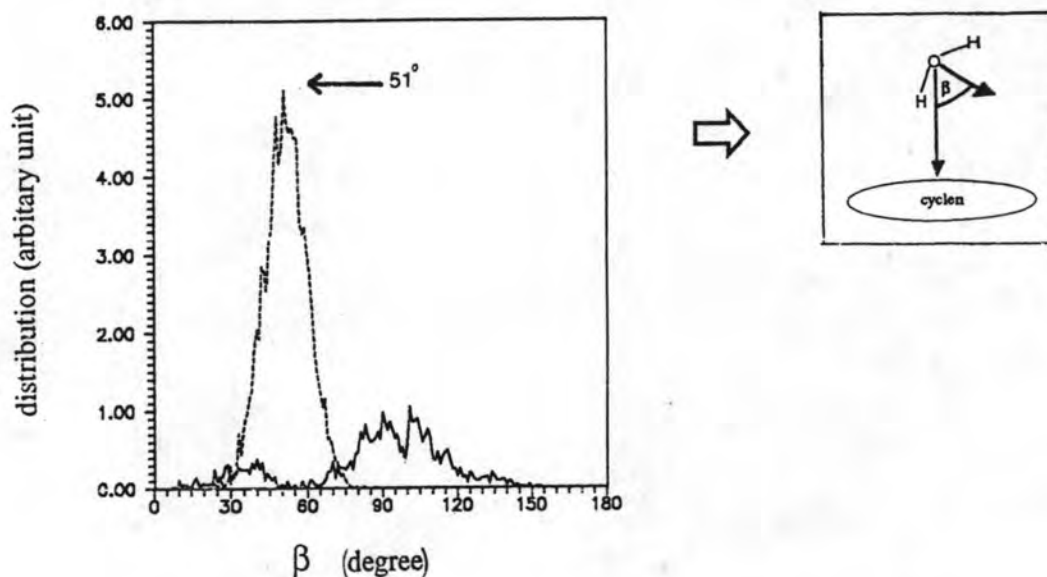
Figure 5.15 Distribution of angle, β, as defined in the attach, for W1 (dashed line) and W2 (solid line), which are situated in the first nearest neighbor site of cyclen.

It is clear from the pronounced peak with a maximum of 51° for W1 that it lies near the z-axis (see Figure 4.3a) and points one O-H bond toward the center of mass of cyclen (an exact value where the O-H bond is along the z-axis is 52.25°). For W2, two possible orientations were exhibited, 7% for 10°≤β≤50° and 93% for 50°≤β≤145°. The corresponding maxima were near 40° and 100°, respectively. However, it has to be kept in mind that these plots were evaluated from the last three million configurations where only one water molecule (W1) is coordinated in the area of the first $g_{EO}(r)$ peak (the 33th-35th millions, Figure 5.12) while W2 is loosely bound to the solvation sphere ranging from 3.4 Å to 4.2 Å.

This water with β ~ 110° was expected to coordinate via a hydrogen bond with the other water, referring to the N-H functional groups of cyclen (detailed investigations are discussed in the next section). Fluctuations of the center-O2 (of W2) distance (Figure 5.13b) and its orientation (Figure 5.15) can be understood by a sort of equivalence between water-water and cyclen-water interactions (Table 5.6). In conclusion, the nearest neighbors of the cyclen molecule have been sketched in Figure 5.16.
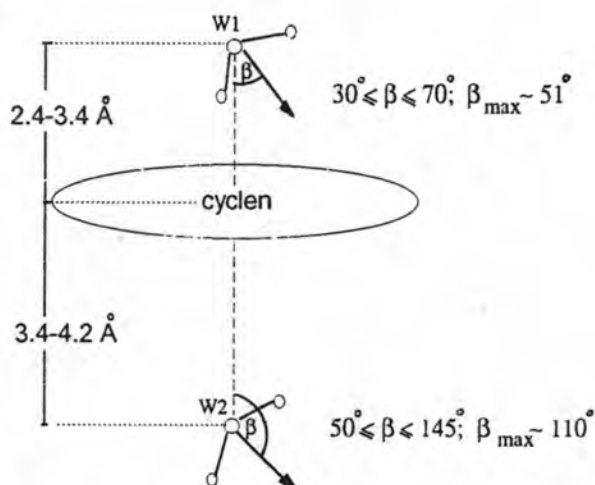
Figure 5.16 Proposed nearest neighbors of the cyclen molecule in a 18.45 mol% aqueous ammonia solution (values taken from the last 3 million out of 35 million configurations of the solution).

The hydrogen bond:

Consider the radial distribution functions referring to the NH functional groups, $g_{NO}(r)$, $g_{NH}(r)$, $g_{H_NO}(r)$ and $g_{H_NO}(r)$ as drawn in Figure 5.17. The distribution of coordination numbers calculated up to the first minima of the corresponding RDFs are plotted in Figure 5.18.

$g_{NO}(r)$ shows a first peak at 3.05 Å, overlapping a second one centered at 3.75 Å. The corresponding integration numbers are 0.8 and 2.6 up to the first and the second minima of 3.30 Å and 4.00 Å, respectively. These numbers agree well with the distribution displayed in Figure 5.18. Since neither peak is well pronounced and the separation between both peaks is not clear cut, it is reasonable to state that these areas contain two water molecules, one for each

peak. The N (of cyclen)-O (of water) distance of 3.05 Å along the N-H bond is found to be identical to that of the N (of cyclen)-O1 (of W1) distance (where W1 is in the configuration given in Figure 4.3a). This result has suggested that an appearance of the first $g_{NO}(r)$ peak is the contribution from W1.
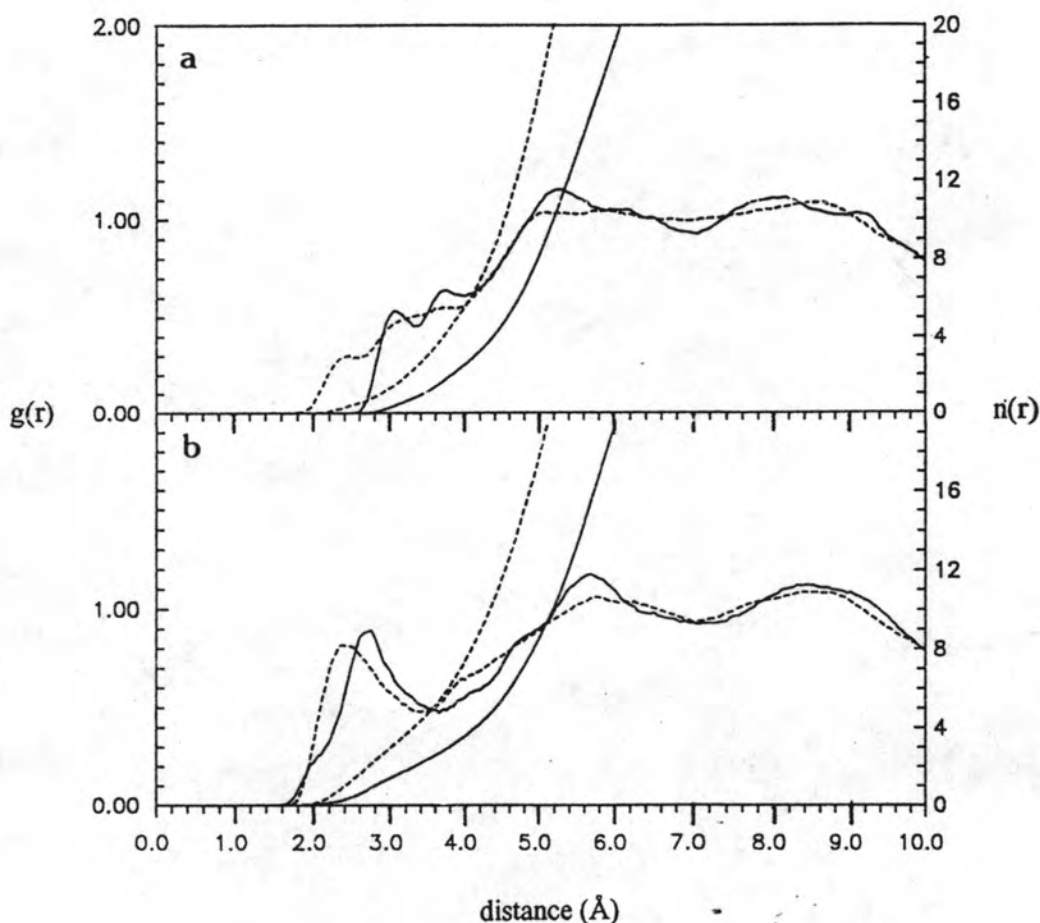

Figure 5.17   Calculated atom-oxygen (solid line) and atom-hydrogen (dashed line) radial distribution functions and running integration numbers for   a) N and   b) H_N atoms of cyclen.
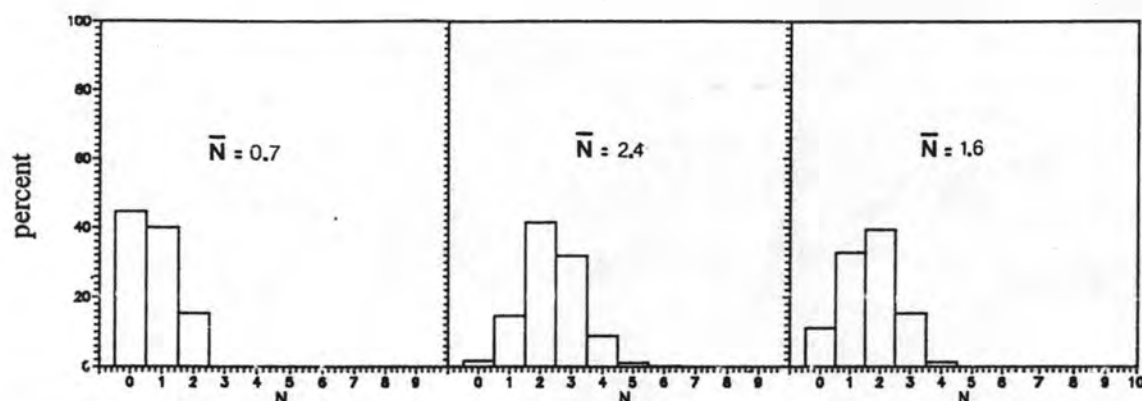
Figure 5.18   Distribution of oxygen atoms of water around the following atoms of
              cyclen, integrated up to r_m of the RDFs,

        a)   N, r_m= 3.30 Å

        b)   N, r_m= 4.00 Å

        c) H_N, r_m= 2.70 Å

A problem arises in the assignment of the correct position for the other water molecule situated under the second peak of $g_{NO}(r)$. It is unusual to report that this water is coordinated to the NH functional group via hydrogen bonding. At this distance, 3.75 Å, hydrogen bonding is no longer valid. To examine this difficulty, distribution of the angle γ, formed by the N-H bond of cyclen and the vector pointing from the nitrogen atom (of cyclen) towards the oxygen atom of water, has been evaluated. Calculations have been made separately for the water molecule centered under the first $g_{NO}(r)$ peak and the other water under the second peak between 3.30 Å and 4.00 Å. The results are plotted in Figure 5.19.

The distribution of the angle γ for water molecules under the first peak of $g_{NO}(r)$ shows a sharp peak at $\gamma = 62°$. This is clearly the O1-N-H or O2-N-H angle, where O1 and O2 are oxygen atoms of W1 and W2, respectively, and N and H refer to atoms of NH functional groups. Therefore, the water molecule under the first peak of $g_{NO}(r)$ is W1 (or W2).

The corresponding curve for the $g_{NO}(r)$ second peak exhibits two maxima, $\gamma = 12°$ and $35°$. These data indicate location of a water molecule (one molecule under this peak) in a "funnel shaped" region, formed by rotating a $50°$ (maximum value of the observed angle) vector, centered on N atom of cyclen, around the N-H bond (of cyclen), with two favourite configurations. The notation W3-W6 is given for this set of water molecules, one for each NH group.
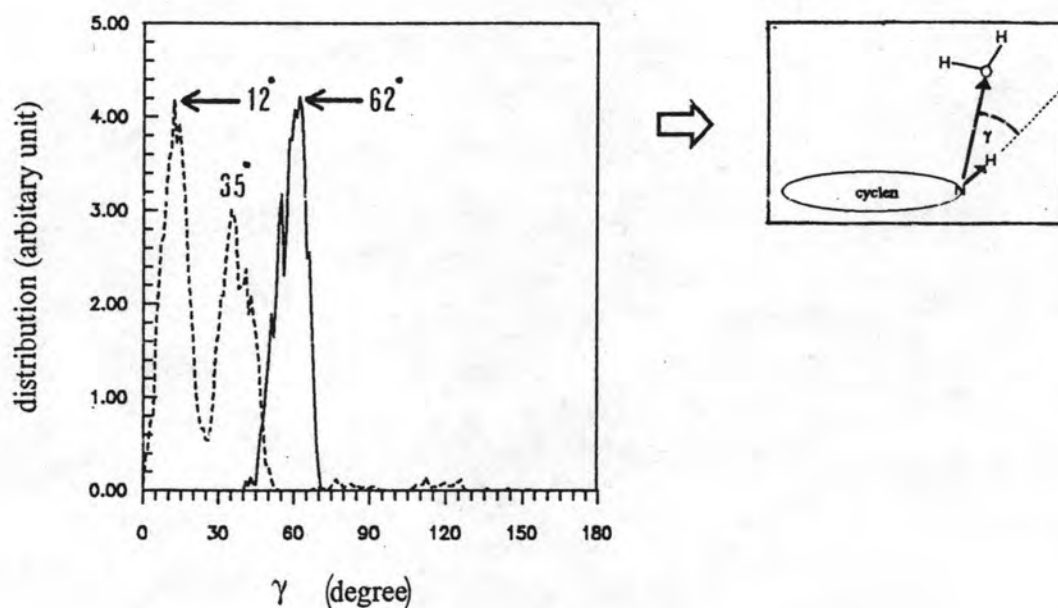

Figure 5.19   Distribution of γ, as defined in the attach, for water molecules lying not further than 3.30 Å from the N atom of cyclen (solid line), and between 3.30 Å and 4.00 Å (dashed line).

A comprehensive investigation of the orientation of W3 (or the others, W4-W6), the distribution of the angle τ, defined by the angle between the dipole moment direction of the water molecule and the vector pointing from its oxygen atom to N (of cyclen) has been carried out. The results are shown in Figure 5.20. The plot shows two broad maxima, $\tau = 64°$ and $133°$, covering from $10°$ to $170°$. This indicates free orientation of W3 (or W4) with two favourite configurations. The data obtained could be clearly understood when the favored configurations were taken from the history file (defined in section (4.3.4)). One of

the 3 million configurations is drawn in Figure 5.21. This picture shows only one of the possible orientations. The rotation of W1 will lead to other equivalent configurations, *i.e.*, alternation of the coordinatation sites is expected to occur. This alternation, caused by the rotation of W1, is suggested to reflect a reorientation of the hydrogen bond from H-O(1)-H-----O(3 or 4)H_2 (Figure 5.21) to H_2O(1)-----H-O(3 or 4)H. Then W3 (or W4) is expected to move along the direction of hydrogen bond. Consequently, the change in the angle γ from one to the other favored configuration, ($\gamma = 12°$ and 35°, as shown in Figure 5.19) can be understood.
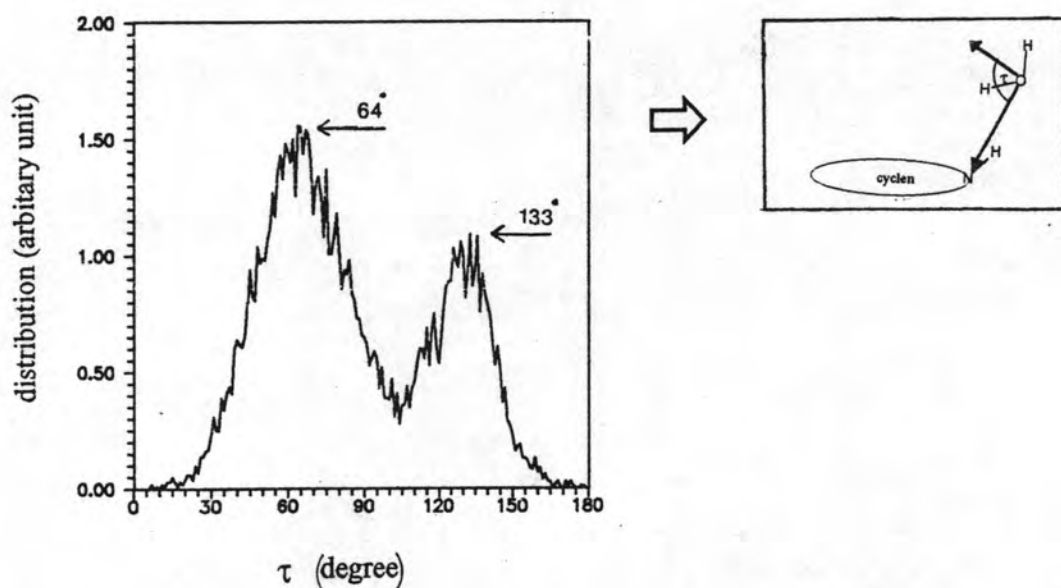
Figure 5.20   Distribution of angle τ, as defined in the attach, for W3
(see text for details).

An asymmetry of both peaks with an integration ratio of about 2:1 could be related to the different favored behaviors of W1 and W2. It also indicates that sampling of 3 million configurations is too small for such dynamic a system.

The N-O(3 or 4) (of W3 or W4) distance between 3.05 Å and 3.75 Å along the N-H bond (maxima of the first two peaks of $g_{NO}(r)$) leads to an the origin-O(3 or 4) distance between 4.76 Å and 5.00 Å. Therefore, the second peak of $g_{EO}(r)$, and hence $g_{TO}(r)$, ranging between 4.00 Å and 5.40 Å, is the contribution from W3-W6. The presence of about 4 water molecules under the second peak of $g_{TO}(r)$, (the integration number up to 5.00 Å of $g_{TO}(r)$ is 6, and that from the first peak is 1.6), is fully consistent with this proposal. These water molecules are not found in the "side" and "plane" regions.

Further confirmation of these observations come from $g_{H_NO}(r)$ and $g_{H_NH}(r)$, depicted in Figure 5.17. The sharp $g_{H_NO}(r)$ peak at 2.75 Å shows the running integration of 2.0 up to 3.30 and of 2.8 up to 3.65 Å. This is surely a contribution from both W1 and W3 (or W4), since the H_N-O1 and H_N-O(3 or 4) distances are the same (see Figure 5.22 for the related distances).
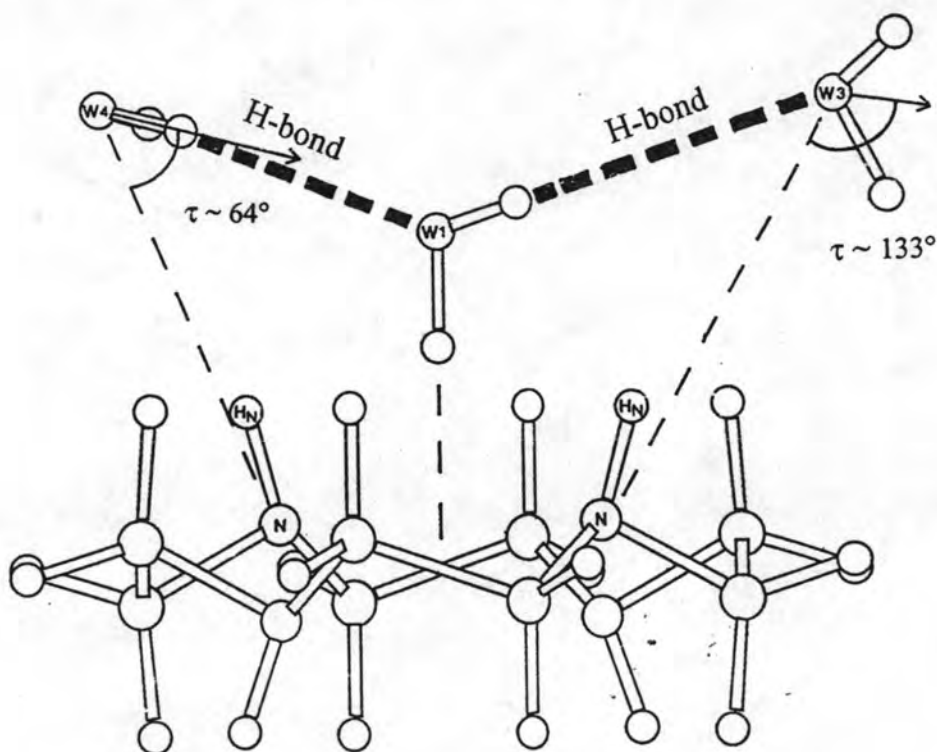

Figure 5.21   The two favourite configurations of W3 incoordinating, via hydrogen bond, with W1 (taken from one, out of 3 million, configurations).
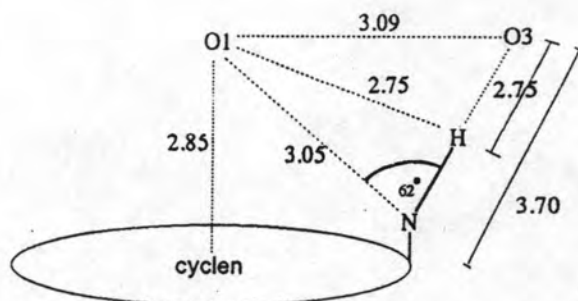
Figure 5.22   Distances and angle between atoms.

The outer hydration shell:

The outer hydration shell is defined, in accordance with $g_{EO}(r)$ and $g_{TO}(r)$, as the solvent molecules lying outside the sphere with a radius of about 5 Å. At this distance, the second peak of the entire and the top regions were included (Figure 5.14a and 5.14b), water molecules in the side and plane regions (Figure 5.14c and 5.14d) and ammonia molecules around cyclen (see the $g_{EN}(r)$ in Figure 5.24) started to be detected, and W1-W6 were not taken into account. Apart from the RDFs in the side and plane regions (Figure 5.14c and 5.14d), information referring to the outer hydration shell could be obtained from those of C, H_C and $H_{C'}$ of cyclen, which are depicted in Figure 5.23.

The arrangement of water molecules in the outer hydration shell has led to pronouced peaks in all the above mentioned Figures. All peaks of the related RDFs cover a distance of some Angstroms, indicating little water affinity and the hydrophobic nature of the CH_2 functional groups. In this region, the RDFs will be mixed with those of other atoms. Therefore, these functions give little orientational information. However, the existence of a peak structure proves that the cyclen molecules still influence the solvent structure significantly up to large distances from the hydrophobic groups.
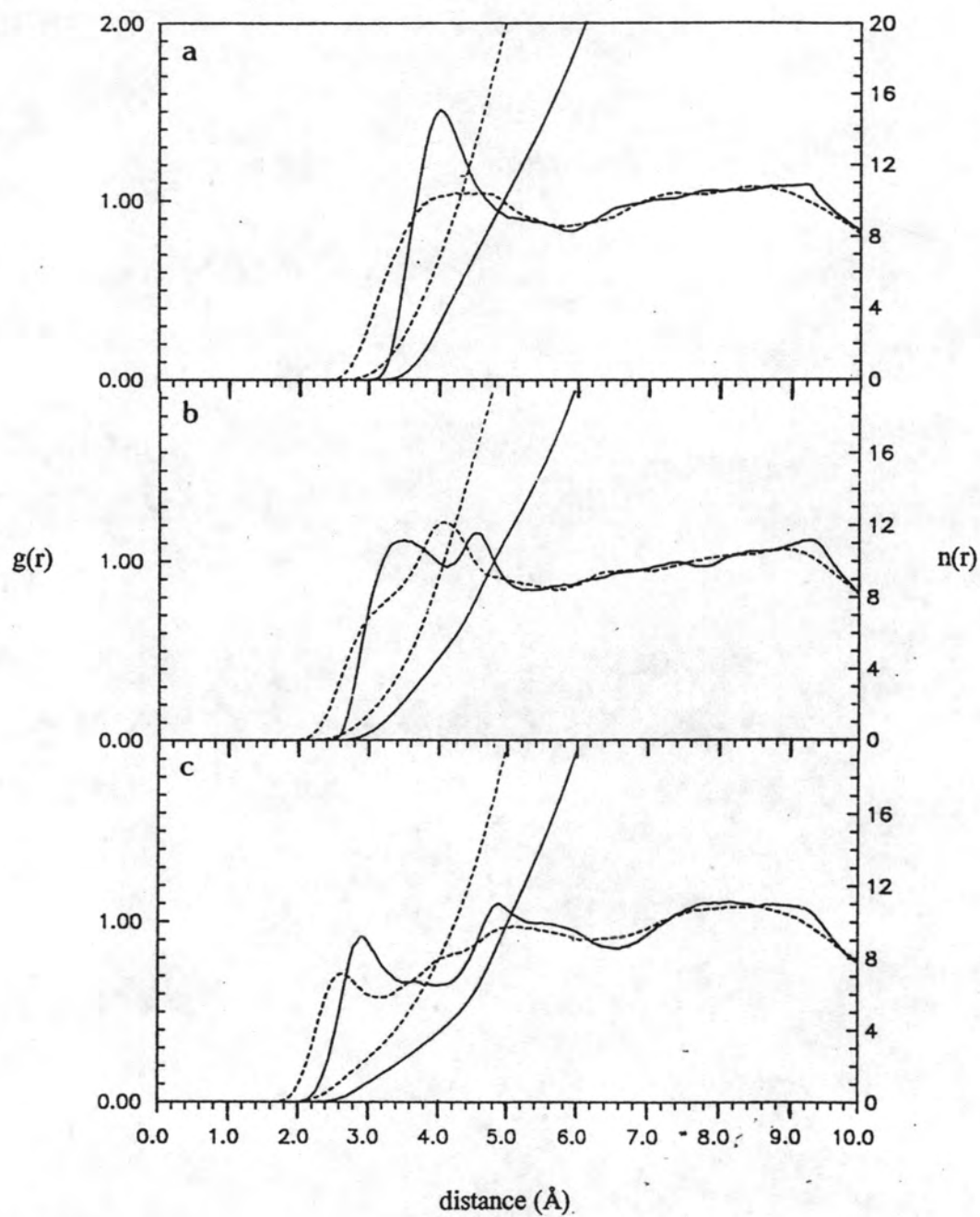
Figure 5.23   Calculated atom-oxygen (solid line) and atom-hydrogen (dashed line) radial distribution functions and running intergration numbers of the (a) C, (b) H_C and (c) $H_{C'}$ atoms of cyclen.

Conclusion for the first-order solvation shell:

Taking into account all the information given and discussed in section (5.3), Figure 5.21 is believed to be a clear picture of the first order solvation shell of cyclen. Due to the symmetry of the ligand, only one half with W1, W3 and W4, has been displayed; the corresponding water molecules, W2, W5 and W6, on the opposite side of cyclen were implicitly included. Characteristics of this model can be summarized as the following:

1.   Symmetric and asymmetric arrangements of W1 and W2 are possible. In the latter case, one of them is removed from its global energy minimum and its behavior, for example flexibility, orientation, the way of forming hydrogen bonds etc., is significantly changed.

2.   W3-W6 lie in a "funnel-shaped" region, centered on N atoms about N-H functional groups, with two favourite configurations. These water molecules form hydrogen bonds with W1 or W2 but not with the N-H groups.

3.   Rotation of W1 and W2 cause alternation of their coordination sites, via hydrogen bonds, with W3-W6.

5.3.3 Ammonia structure around cyclen molecule

Radial distribution functions and running integration numbers for ammonia molecule referring to center of mass, to NH and CH_2 functional groups were plotted in Figures 5.24, 5.26 and 5.27, respectively. Distribution of coordination numbers of the first one was given in Figure 5.25.

Running integration numbers of 2.8 up to 7.00 Å of the first pronounce $g_{EN}(r)$ peak is the contribution from the distribution plot given in Figure 5.25 (N=3.0 in this Figure, which is differ from 2.7 obtained from the integration in Figure 5.24, because they were calculated from different numbers of configurations, 3 and 28 millions, respectively). It was observed from looking through the history file that these ammonia molecules are always coordinated to the inner hydration shell (W1-W6) of cyclen. One of the mentioned configuration was extracted and monitored in Figure 5.28. They are also contributed to the first $g_{H_wN}(r)$ peck at 5.40 Å, since its running integration numbers of 2.9, equivalent to those of $g_{EN}(r)$. The conclusion which seems reasonable is to assign these

ammonia molecules as the solvation shell of cyclen, coordinated to the "inner water shell" of ligand.
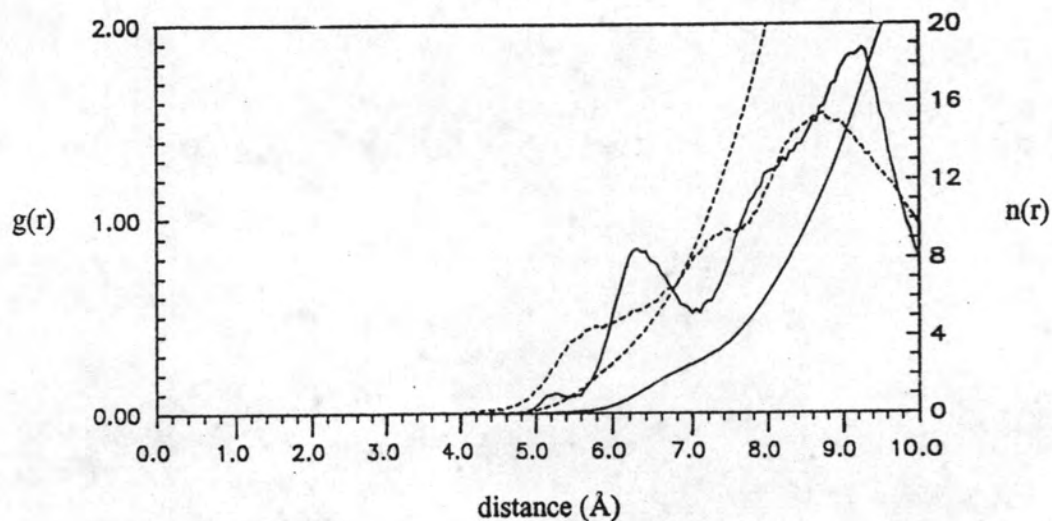

Figure 5.24   Center-nitrogen (solid line) and center-hydrogen (dashed line) radial distribution functions and corresponding integration numbers.
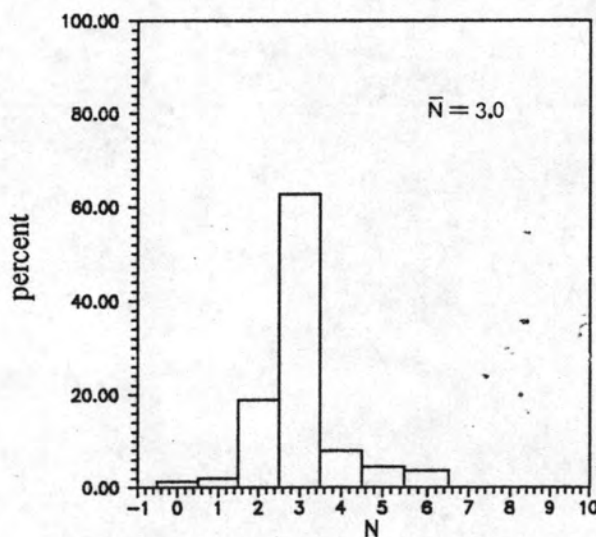

Figure 5.25   Distribution of nitrogen atoms of ammonia around center of mass of cyclen, integrated up to the first minimum of 7.00 Å of the $g_{EN}(r)$.
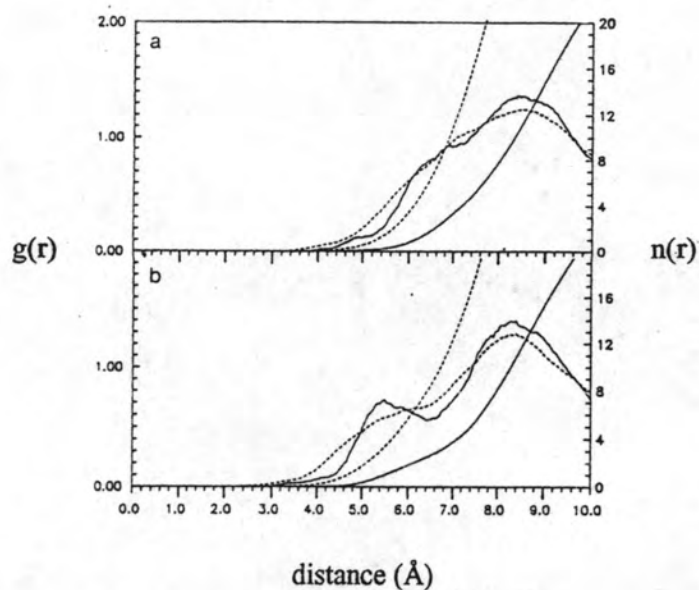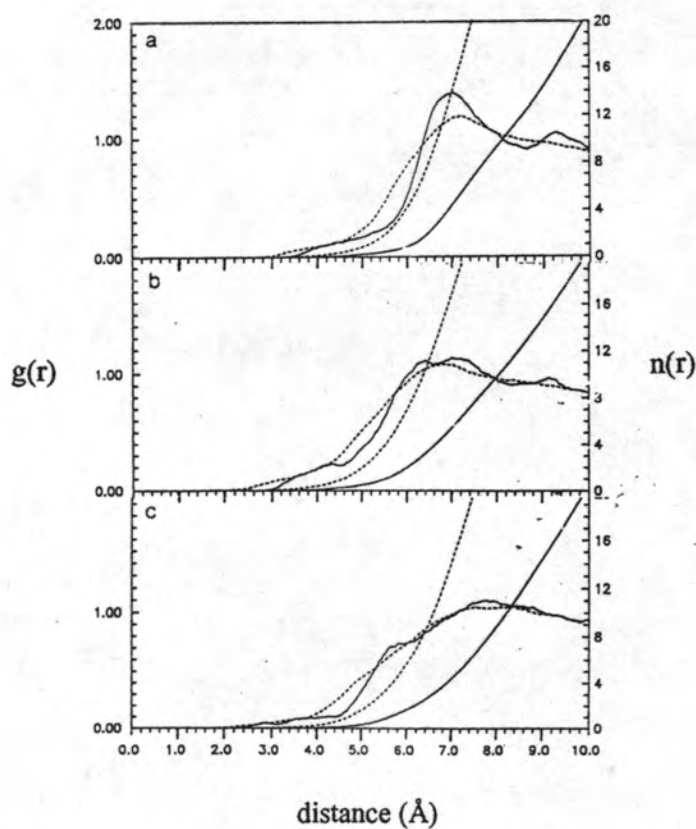
Figure 5.26   Atom-nitrogen (solid line) and atom-hydrogen (dashed line) radial
distribution functions and corresponding integration numbers for the
a) N and   b) H_N atoms of cyclen.

Figure 5.27   Atom-nitrogen (solid line) and atom-hydrogen (dashed line) radial
distribution functions and corresponding integration numbers for the
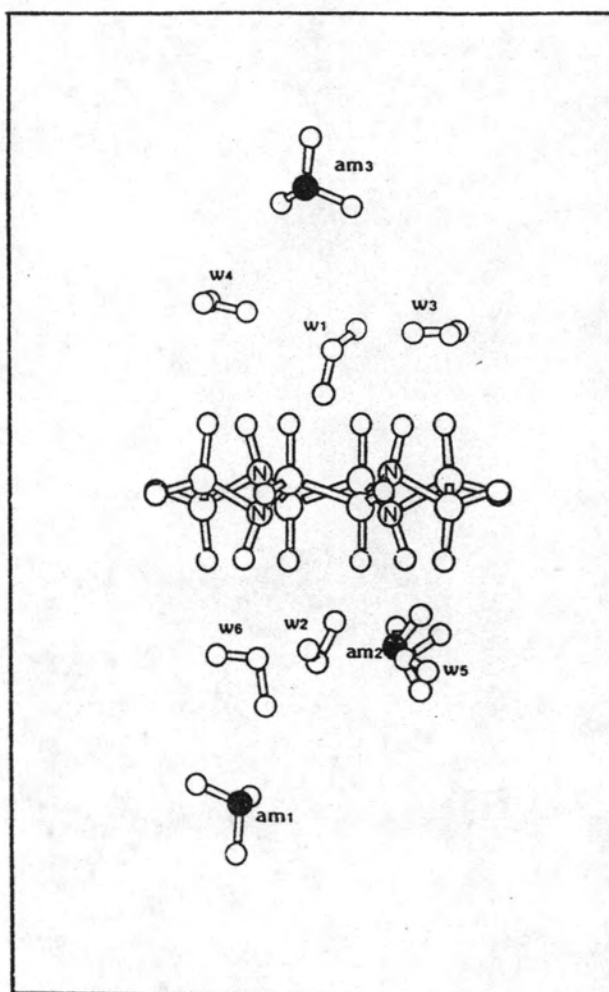a) C and   b) H_C and   c) $H_{C'}$ atoms of cyclen.

Figure 5.28   One out of 28 million configurations of the solvation shell of cyclen consisting of 6 water and 3 ammonia molecules.